Available online at www.sciencedirect.com
ScienceDirect
Tectonophysics 466 (2009) 427–437
TECTONOPHYSICS
www.elsevier.com/locate/tecto

Non-catastrophic landslides induced by the M_w 7.6 Chi-Chi earthquake in central Taiwan as revealed by PIV analysis

Chia-Han Tseng [a], Jyr-Ching Hu [a,*], Yu-Chang Chan [b], Hao-Tsu Chu [c], Jin-Fa Lee [c], Jheng-Yue Wei [c], Chia-Yu Lu [a], Ming-Lang Lin [d]

[a] Department of Geosciences, National Taiwan University, Taipei, Taiwan
[b] Institute of Earth Sciences, Academia Sinica, Taipei, Taiwan
[c] Central Geological Survey, Taipei, Taiwan
[d] Department of Civil Engineering, National Taiwan University, Taipei, Taiwan

Available online 22 November 2007

Abstract

The Chi-Chi earthquake occurred in the western foothills of central Taiwan, which triggered coseismic and catastrophic Chiufengershan dip-slope landslides, Tsaoling rockslides and surface stripping of the Jiujiufeng area. After a few days of the Chi-Chi event, the Hongtsaiping area in central Taiwan was reported to have several meters of slide in a small scale area. The reported landslides are dissimilar to the catastrophic events. To better understand the characteristics of such non-catastrophic and unobvious landslide, we try to characterize in detail the sliding directions, their magnitudes and region of the landslide. We analyzed three orthorectified aerial photographs of the Hongtsaiping area, which were taken in 1998/06/13, 1999/11/18 and 2002/10/26, using the Particle Image Velocimetry (PIV) technique. Through the method we correlated the image pixels of the two aerial photographs in order to derive the displacement vector field. The results of the PIV analysis have helped us not only find the areas where sliding had happened, but also evaluate the azimuth and magnitudes of the sliding event. The PIV analysis in the Hongtsaiping area covers a dimension of about 3228 × 2448 pixels in an area of about 1.2 km^2. Our results show that the maximum horizontal displacement of the landslide is about 24 m towards NW in the study area. This unobvious but wide-coverage landslide may need further investigation in mechanisms combining with available or new geological data.

Keywords: Chi-Chi earthquake; Non-catastrophic landslides; Orthorectification; Particle Image Velocimetry (PIV)

1. Introduction

On September 21, 1999, the Chi-Chi earthquake whose epicenter is at 23.85°N, 120.81°E struck central Taiwan. Because of the moment of magnitude of M_w 7.6 there were more than 2400 people killed in this event, and properties were enormously damaged around the island (Kao and Chen, 2000; Angelier et al., 2001; Chen et al., 2001a,b; Lee et al., 2002). After the Chi-Chi earthquake, Chiufengershan dip-slope landslides, the Tsaoling rockslides (Hung, 2000; Hung et al., 2000; Lin et al., 2000; Liao et al., 2002; Chigira et al., 2003; Shou and Wang, 2003), surface stripping of the Jiujiufeng (99 peaks) and the Hontsaiping landslide took place due to this event. The size of the Chiufengershan dip-slope landslides was about 200 ha in area and 36 million m^3 in volume, which is composed of shale and sandstone, and the landslide debris dammed two small streams, whose total volume of the two dam-up lakes is 1.9 million m^3. In the Tsaoling rockslides, a rock mass of shale and muddy sandstone about 120 million m^3 slid down the dip slope. Only 20% (about 25 million m^3) of the sliding mass dropped into the valley of the Chingshui river covering the river as long as 5 km. Trees and grass covered Jiujiufeng initially, but after the Chi-Chi earthquake the stripping, that is the removal of all the trees and grass, took place during the earthquake shaking.

In addition to the obvious and catastrophic landslide events, many observations and reports (Lee et al., 2004; Wei and Lee, 2006) by researchers and local residents show that there were also other types of landslides occurring in central Taiwan in

* Corresponding author. Tel: +886 2 33662943; fax: +886 2 23636095.
E-mail address: jchu@ntu.edu.tw (J.-C. Hu).

0040-1951/$ - see front matter © 2007 Elsevier B.V. All rights reserved.
doi:10.1016/j.tecto.2007.11.019

addition to the above-mentioned catastrophic landslides after the Chi-Chi earthquake. The barely noticed landslide, the Hongtsaiping landslide is located at central Taiwan, about 15 NNE of the epicenter (Fig. 1). The landslide affected region was measured to be around 1500 m × 800 m in dimension with displacement of several meters up to tens of meters. The non-catastrophic phenomenon was reported by local residents about 3 to 5 days after the Chi-Chi earthquake.

In order to better understand the non-catastrophic landslide phenomenon, we apply displacement detection technique to measure the overall displacement pattern. The Particle Image Velocimetry (PIV) technique is originally used for hydromechanics field with the advantage of analyzing displacement of images of flow with the cross-correlation method. Thus, we take the advantage to measure such non-catastrophic landslides with the PIV technique to better understand its direction and magnitude of displacement. Some researchers have applied multi-temporal aerial and satellite images for studying the spatial and temporal evolution of landslides (Dominguez et al., 2003; Delacourt et al., 2004; Casson et al., 2005) with good results, and other researchers also successfully use the PIV method to analyze impulse waves generated by landslide (Fritz, 2002). Similar to PIV technique, some other studies have shown the potential of multi-temporal image correlation for mountains glaciers characteristics (Kääb, 2002; Berthier et al., 2005). This technique is also applied to characterize the displacement fields in a granular material subjected to extended shear (Chambon et al., 2003).

In this study, at first, we want to observe and analyze the unobvious and the non-catastrophic Hongtsaiping landslide different from other catastrophic landslides, so we obtain three monochromatic aerial photographs of the Hongtsaiping area (the Taiwan Grid 67, 1:5000, pixel size of 0.375 m) acquired from Central Geological Survey (CGS) and Chinese Society of Photogrammetry & Remote Sensing (CSPRS) which are taken in 1998/06/13, 1999/11/18 and 2002/10/26. Then we orthorectify them in order to correct the geometric distortion of photographs and to give them geographic coordinate. Finally, by means of the cross-correlation method in the PIV technique, we can obtain the direction and magnitude of displacement in the Hongtsaiping landslide area.

2. Geological background of the Hongtsaiping area

According to the geological map compiled by the Central Geological Survey (Fig. 2), the study area is located at inner

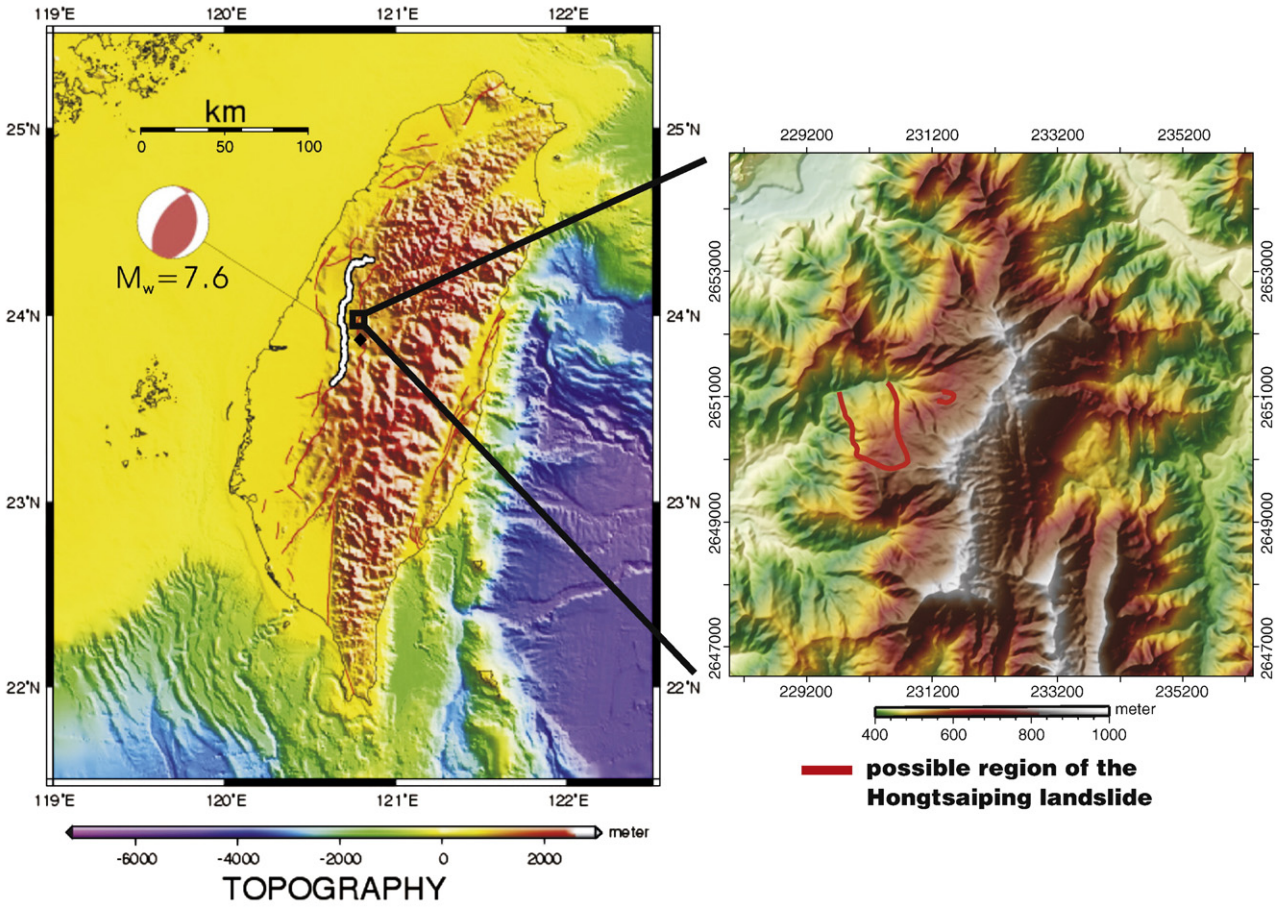

Fig. 1. The Hongtsaiping landslide area. It is triggered by the Chi-Chi earthquake (M_w=7.6, 1999) is located in central Taiwan, about 19 km north of the epicenter on the left topographic map (white thick line represents the Chelongpu Fault). In the color DEM on the right (Digital Elevation Model, pixel size of 20 m), the study area is bounded by red line, and the elevation is from about 500 m to 800 m, and the area is about 1.2 km^2 (1500 m × 800 m). The slope is about 19° toward NNW. (For interpretation of the references to colour in this figure legend, the reader is referred to the web version of this article.)

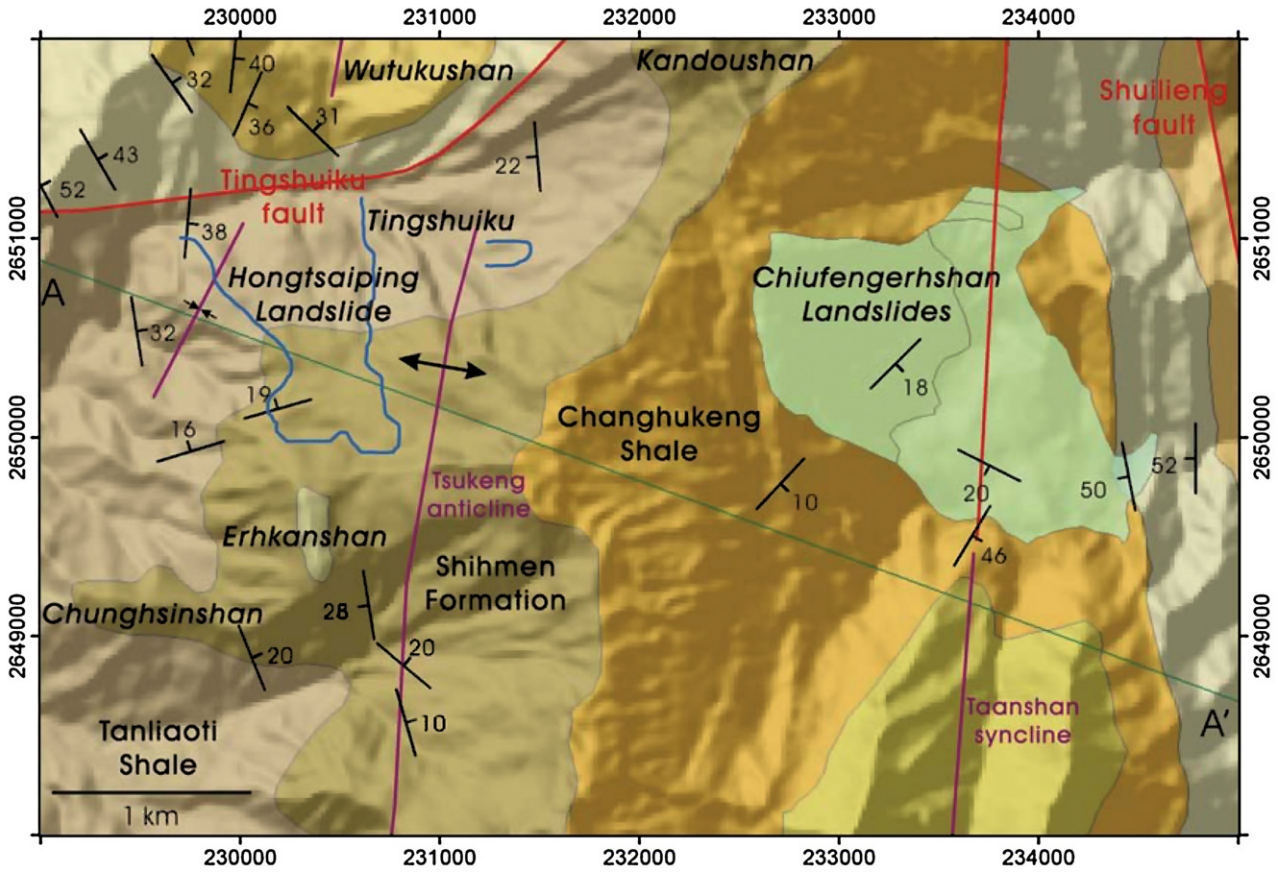

Fig. 2. The geological map (from Central Geological Survey) of the Hongtsaiping landslide area. The landslide area is mainly at the left limb of Tsukeng Anticline, and the right limb of a small syncline. The north boundary of the landslide area is Tingshuiku Fault, and a creek passes along this fault flowing to the west. Chiufengershan landslide is about 2.5 km east of the landslide area.

foothill zone, and is underlain mainly by Miocene sedimentary rocks. The strata exposed in this study area are, in a younging order, the Tanliaoti Shale, the Shihmen Formation, the Changhukeng Shale, and the Shenkeng Sandstone. The Tanliaoti Shale consists mainly of massive gray shale with thin-bedded sandstone. The Shihmen Formation is composed of 3 layers of thick sandstone. The Tanliaoti Shale is distributed in the lower part of the landslide area and the Shihmen Formation is distributed in the upper part of the landslide area. The Changhukeng Shale is composed of dark gray marine shale with subordinate sandstone with ripple marks on the bedding surface. The Shenkeng Sandstone, which usually forms cliffs, is composed of massive sandstone with dark gray shale.

In tectonics, there is an anticline, called the Tsukeng anticline, in the southeast of the landslide area, and the azimuth of the left limb is N135°W, 19°N. Thus, it is inferred that the Hongtsaiping landslide is a dip-slope landslide with relatively small movement. This landslide area is about 1.2 km^2 (1500 m × 800 m), and the northern boundary is cut by a creek and a fault, called the Tingshuiku fault. Along this creek, we found bending of layers at the foot of the slope (Fig. 3) and a main scarp (Fig. 4) which supports the sliding of the formations in this area. Also, breaking of roads and bended stems of betel palms are commonly observed in this study area suggesting unstable ground movement.

3. Methods of analysis

Before evaluating the magnitude and direction of the displacement of the Hongtsaiping landslide area, we orthorectified three monochromatic aerial photographs in order to correct the geometric distortion of the photographs and to give them geographic coordinate (in this case, the Taiwan Grid 67) and pixel resolution of 0.61 m/pixel for the PIV analysis. After that, we applied the cross-correlation method in the PIV technique to analyze the displacement of the Hongtsaiping landslide area in the selected images.

3.1. Orthorectification technique

Because there is geometric distortion in the aerial photographs, we have to rectify them by means of orthorectification which is a mathematical process of removing the geometric distortion caused by relief of ground objects and camera in a photograph. The scale of these photographs is 1:5000 and the original resolution is 0.375 m/pixel.

When rectifying geometric distortion in a photograph or an image, we have to know the relationship between the spatial coordinates in the image and those on the Earth's surface. Ground control points (GCPs) are necessary information on the Earth's surface to determine the relationship, so the GCPs data

Fig. 3. Bending at the foot of the slope. It is a fault gauge and breccias of the Tinshuiku fault (modified from Lee et al., 2004). Lower sketch characterizes the structure which has round edge of the most front part.

(read from the 1/5000 photo base map which is measured by Aerial Survey Office, Forestry Bureau) have to be acquired before we start to rectify these images. The coordinates of a point in the image (x_i, y_i) are functional with those of the corresponding point on the surface (x_i, y_i), so we can express the relationship as (Rees, 2001)

$$x_s = f(x_i, y_i) \quad \text{and} \quad y_s = g(x_i y_i). \tag{1}$$

The relationship is a general linear model which are represented as following equations:

$$x_s = a_1 + a_2 x_i + a_3 y_i \quad \text{and} \quad y_s = a_4 + a_5 x_i + a_6 y_i. \tag{2}$$

Because each GCP provides two pieces of information, an x-coordinate and a y-coordinate, in general 3 GCPs are sufficient to determine the relationship. However, we still used more than 3 GCPs to avoid random errors which may occur during the process. To determine the proper values of prior 6 parameters ($a_1 \sim a_6$), a least-square fitting procedure is carried out.

We hope to change actually the geometry of the image, so that if conforms to the chosen coordinate system (x_s, y_s). In general, we can define a relationship of transformation as follows:

$$i = F(i', j') \quad \text{and} \quad j = G(i', y') \tag{3}$$

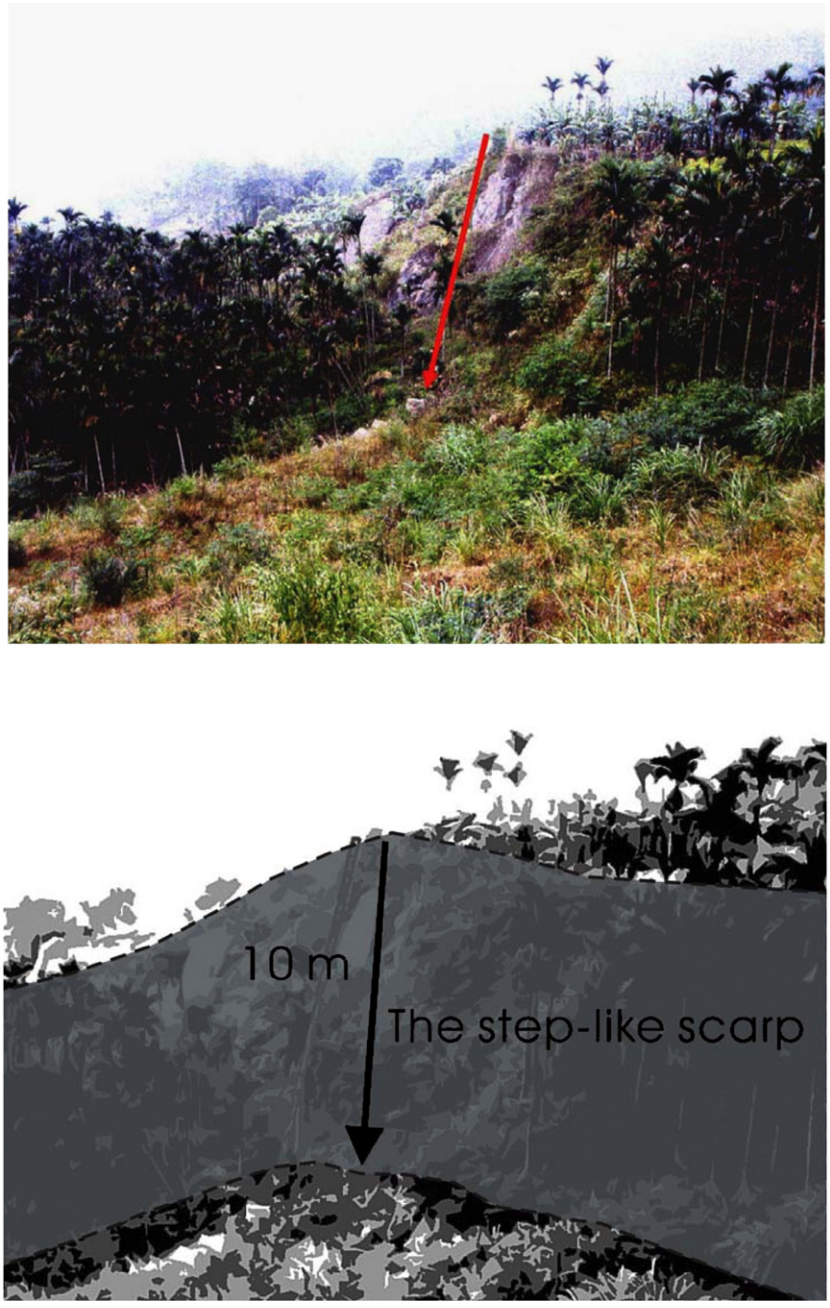

Fig. 4. Upper main scarp of the Hongtsaiping landslide, whose vertical displacement about 15 m (Lee et al., 2004). Lower sketch accounts for that the step-like scarp extends widely.

where (i,j) are the pixel coordinates in the untransformed image, (i',j') are those in the transformed image, and the functions F and G can be derived from the functions f and g in Eq. (1). Eq. (3) can find the pixel coordinate (i,j) in the original untransformed image which would be copied into a point (i',j') in the new image. The pixel coordinates are only defined for integer values of the column and row numbers i and j, but non-integer values would be resulted from Eq. (3). If this happens, we need the resampling technique, so that we can choose the pixel value from the original image to copy into the new image.

The simplest technique of resampling is nearest-neighbor resampling. We just identify the pixel in the original image which is spatially nearest to the calculated position (i,j), and then copy its pixel value to the location (i',j') in the new image. This approach has the advantage that it does not alter any of the pixel values. However, it can produce resampled images which have jagged edges. So if we want to obtain smoother results, interpolation can be used. The pixel value copied into the new location (i',j') is a weighted average of the pixel values in the neighborhood of the calculate location (i,j). The commonest forms are bilinear interpolation, which uses a 2×2 pixel neighborhoods, and bicubic interpolation, which uses 4×4 pixel neighborhoods.

Orthorectified images have less relief displacement and geometric error than non-orthorectified images, and thus they

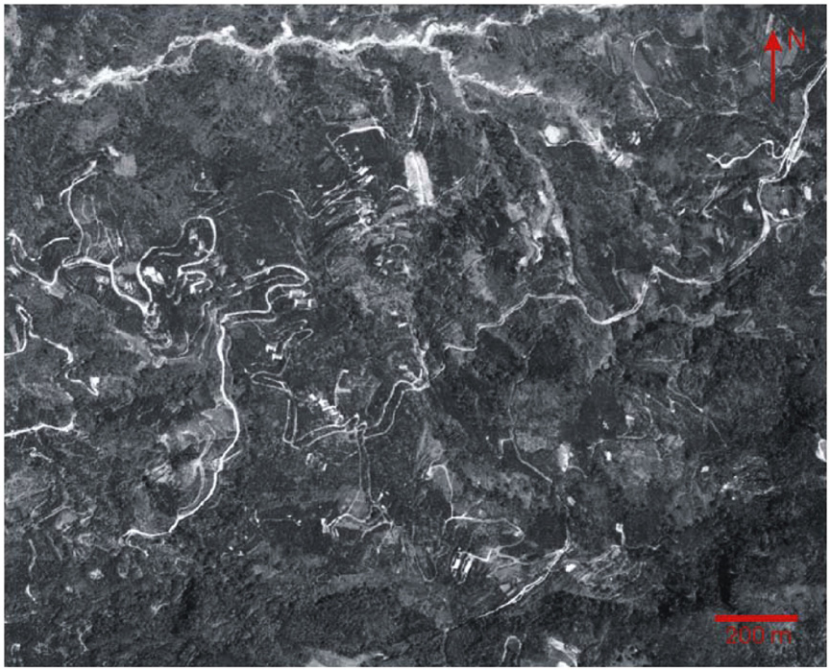

Fig. 5. PIV overlaps two input images and makes them transparent before analyzing. The obvious displacement of roads and other objects can be observed clearly in the central part of this image.

are considered more accurate. In this study, we use single photo, DEM to rectify the images and choose 10 GCPs in the non-displacement area, and the error from orthorectification is about 1.5 m (~2.5 pixels).

3.2. Particle Image Velocimetry (PIV)

Particle Image Velocimetry (PIV) is whole-flow-field technique providing instantaneous velocity vector measurement in a cross-section of a flow (Landreth and Adrian, 1988; Adrian, 1991; Lecordier and Mouqallid, 1994; Rees, 2001; Rhoály et al., 2002). In addition, some studies applied PIV technique for producing displacement map from multi-temporal images (Chambon et al., 2003). With this feature, we use PIV to analyze the movement of a fine mesh of the monochrome aerial photograph patch.

After orthorectifying, PIV overlaps the two rectified images with all the same area. From the overlapped image (Fig. 5), we can clearly see that the roads and other objects displace from its original position to another and the trend of the displacement is towards NW. The procedure of the PIV analysis is shown as flowchart (Fig. 6).

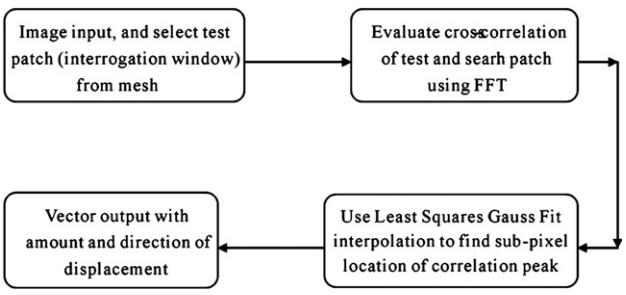

Fig. 6. The flowchart of PIV analysis. PIV has four steps in its procedure and we can set parameters in any one of them to improve the results of analysis.

In order to attain more accurate and precise results, the cross-correlation method which is a standard one of estimating the degree to which two series are correlated is the one of the methods for PIV to evaluate the displacement of every pixel which may include roads, trees, rocks, houses and so on, and each has its own gray value distinguish itself from others. To reduce the computational requirement, the correlation operations are conducted in the frequency domain by taking the fast Fourier transform (FFT) of each patch and following the convolution theorem. The equation for the cross-correlation is:

$$C(s) = \int\int_{\mathrm{IA}} I_1(X) \cdot I_2(X+s)dX. \quad (4)$$

Where $C(s)$ means the degree of correlation, or the degree of match, I_1 and I_2 are interrogation area (IA, Chrominance matrix), and s is displacement.

The cross-correlation of $I_1(X)$ and $I_2(X+s)$ is evaluated, and normalized by the square root of the sum of the square values of $I_2(X+s)$ over the range of X occupied by the test I_1 patch. The resulting normalized correlation plane $C(s)$ indicates the "degree of match" between the test and search (I_2) patch over the offset range in the domain of s. The correlation plane $C(s)$ is evaluated at single pixel intervals. By fitting a Least Square Gauss Fit interpolation to the region close to the integer peak, the displacement vector is established to sub-pixel resolution. To improve the resolution, a smaller interval can be selected, with a corresponding increase in computational burden. The RMS (Root Mean Square) error of the cross-correlation is about 0.3 pixels.

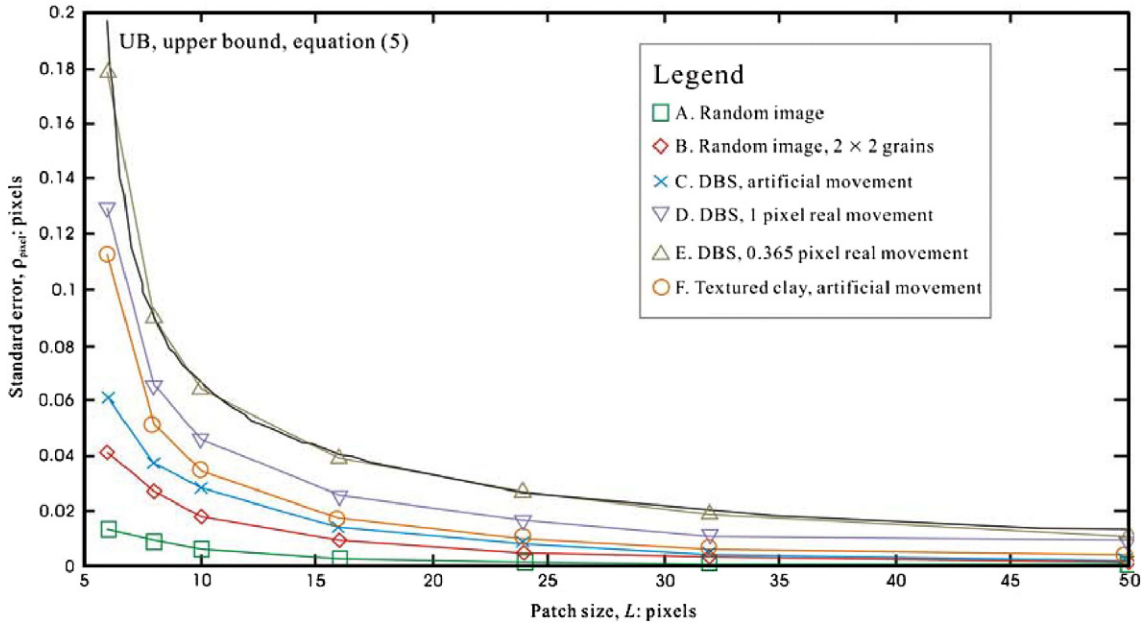

Fig. 7. PIV precision against patch size. Every single test is almost consistent to Eq. (5) (edited from White et al., 2003), and it tells that the smaller patch size we set, the more precise results we can get.

The patch size consists of a matrix of randomly generated pixel intensities, in the range 0 to 255. This random image allows subjects movement to be exactly controlled, and makes it possible to remove any image changes due to lighting or camera shake. A series of seven PIV analyses were conducted, in which the entire 3228×2448 pixels random image was covered in square patches with side length, L, 8, 16 and 32 pixels respectively. Each PIV analysis revealed a scatter of values, distributed close to zero. Large PIV patches produced less scatter, and therefore improved precision. By plotting the standard deviation in measured displacement against test patch size, the influence of patch size on measurement precision can be seen (Fig. 7). Curve A shows the results from the seven PIV analyses of the random image, revealing a precision better than 0.01 pixels for patches greater than 8×8 pixels in size. The largest PIV patches, of size 50×50 pixels, were distributed around zero with a standard error of 0.0007 pixels. In order for these analyses to be a test of the measurement precision rather than the measurement resolution, the sub-pixel correlation peak was evaluated at intervals of 1/10,000th of a pixel, rather than 1/200th.

This series of validation experiments reveals that the precision of PIV is a strong function of patch size, and is also influenced by image content. The empirically derived curve UB in Fig. 7 is an upper bound on the precision error, ρ_{pixel}, and is given by equation: (White et al., 2003)

$$\rho_{\text{pixel}} = 0.6/L + 150000/L^8. \quad (5)$$

Where ρ_{pixel} is the precision error determined by the image width in pixels, and L is patch size. This equation allows a conservative estimate of the random error present in subsequent PIV data to be made.

4. Discussion

4.1. The results from the PIV analysis

As the results shown by PIV, we can see the horizontal direction and magnitude of the Hongtsaiping landslide in two different time intervals respectively (Fig. 8). In Fig. 8A and B (between 1998 and 1999, 1998 and 2002, respectively), they show approximate the same landslide area, about 1500 m×800 m, and the same directions, about N45°W in southern part and N25°W in northern part (Fig. 9). The largest magnitude in few areas is about 28 m (~46.28 pixels) in Fig. 8A, and 24 m (~39.34 pixels) in Fig. 8B. The definite area of the Hongtsaiping landslide can also be clearly shown by the magnitude image (Fig. 10). Taking the result between 1998 and 2002 for example, the boundary can be viewed as the border between light blue and green, which is also the displacement value 3.5 pixels. Comparing this value to the error from orthorectification about 2.5 pixels and to the RMS error (0.3 pixels) from the cross-correlation (Meinhart et al., 1999), we can know that PIV can precisely find real displacement area, as well as the magnitude of displacement. Beside the main Hongtsaiping landslide area, about 500 m east of the main study area, there is a minor landslide which is about 10 m in maximum toward west and the area is about 200 m×100 m. It can also be seen in Fig. 8A and B. Generally, the magnitude larger than 10 m is about 43%, while that less than 5 m is about 54%. Since these results are expressed in horizontal component, if we want to know the magnitude parallel to the slope of bedding, we can multiply the dip angle (19°) of secant of the bedding in this study area. As a result, the approximate amount of displacement is about 25 m, which would be more consistent to really local condition. PIV also has 6 different algorithms to

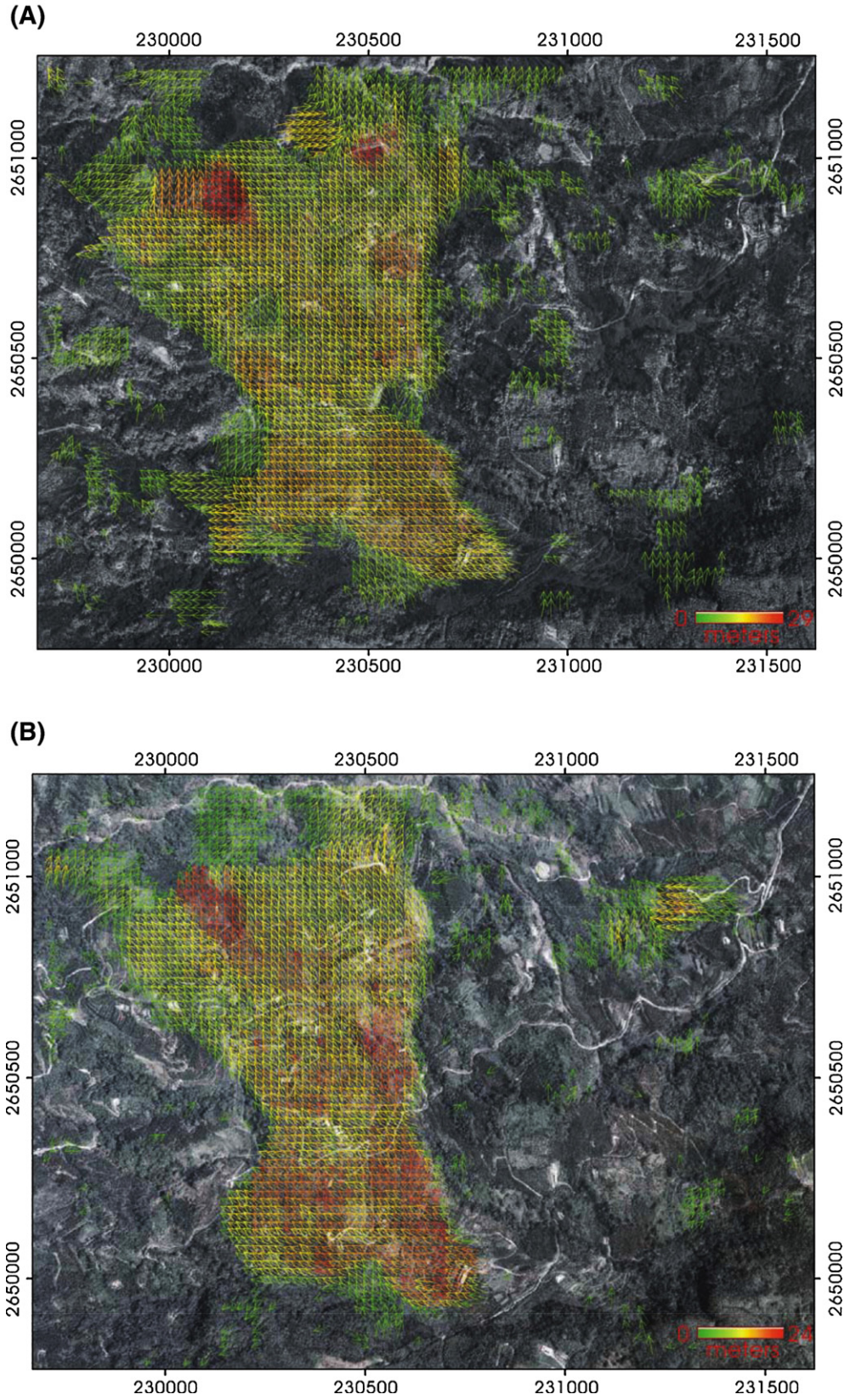

Fig. 8. The results of the Hongtsaiping landslide including direction and magnitude of displacement. Green color means little to zero displacement, and red means large one. Outside of main landslide area there are vectors in many places due to the effect of image appearance. (A) Result between 1998 and 1999. (B) Result between 1998 and 2002. (C) Result between 1999 and 2002. Both of the results in A and B show that the directions of displacement are consistent. In the north part, displacement is toward NNW, while it is toward NWN. The result in C shows that there is no displacement in the main landslide area except some small areas due to the local topography which easily induces landslide or creep. (For interpretation of the references to colour in this figure legend, the reader is referred to the web version of this article.)

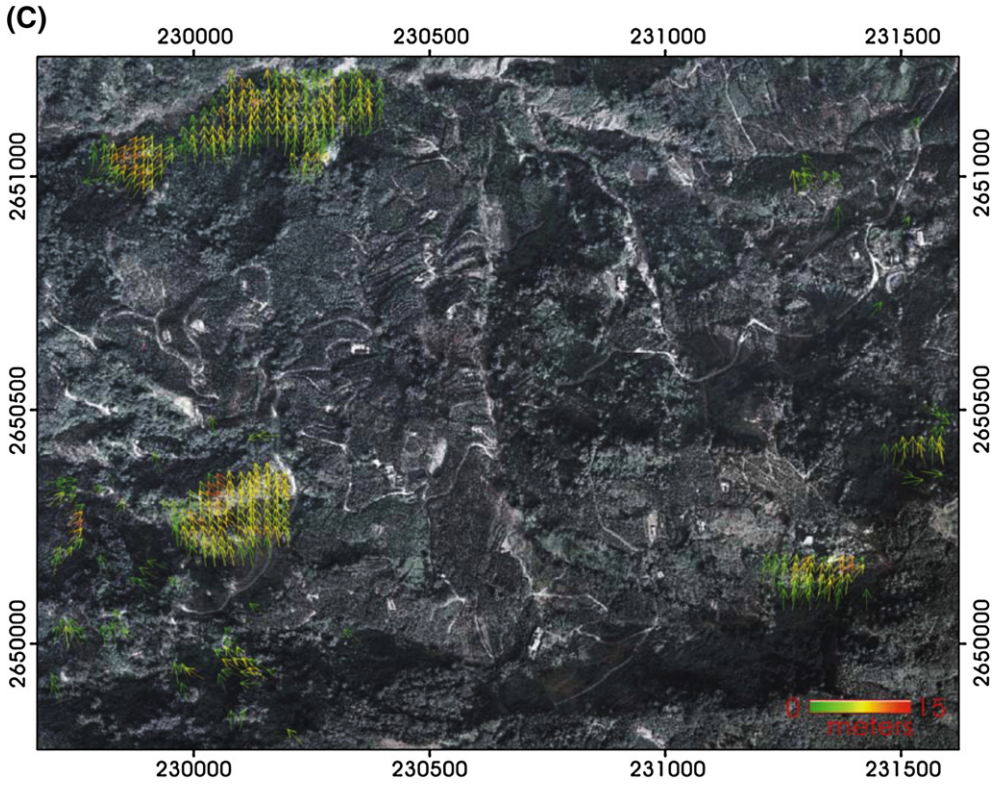

Fig. 8 (*continued*).

detect peak value (Fig. 11), and here we selected proper one to present the results. As for the result between 1999 and 2002, the main landslide area does not show any displacement (Fig. 8C). In other words, the Hongtsaiping landslide did not take place again between 1999 and 2002.

4.2. Factors affecting the PIV precision

There are three important factors on the PIV precision: (a) patch size, (b) appearance, and (c) displacement distance: whole or fraction of a pixel. The factor of patch size discussed

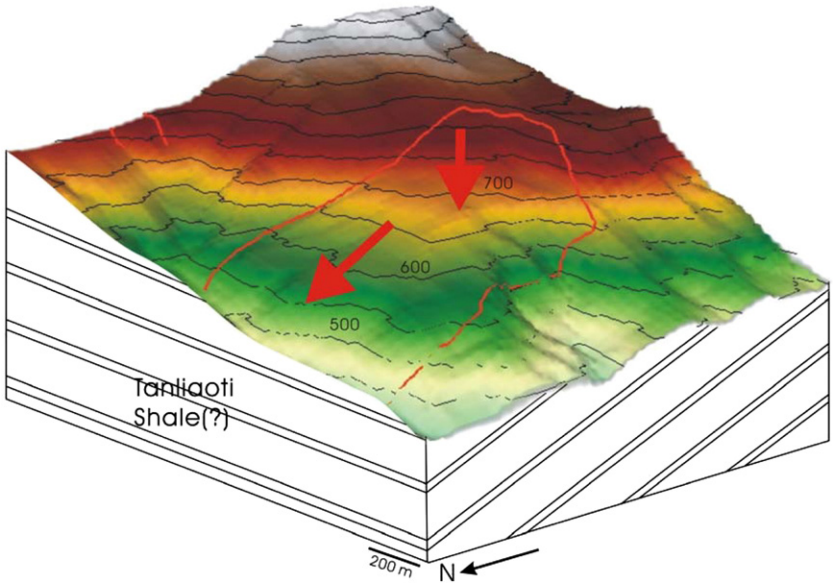

Fig. 9. Topography of the Hongtsaiping landslide area and cross-section of underground structure (unsure). Two red arrows indicate the directions of displacement which are different in southern and northern part, possibly because the direction of slope is different in these two parts. (For interpretation of the references to colour in this figure legend, the reader is referred to the web version of this article.)

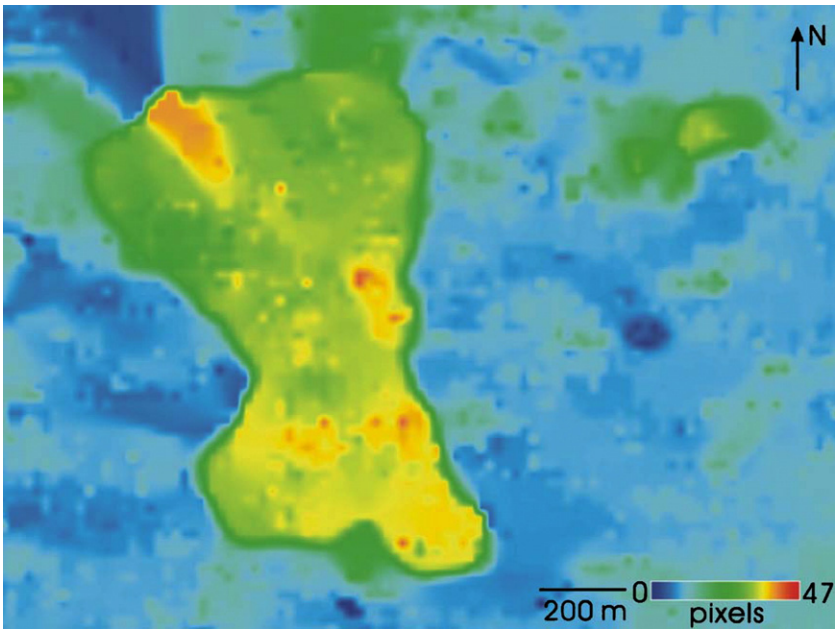

Fig. 10. The Hongtsaiping landslide area shown only in magnitude. The boundary between green and blue can account for the possible landslide area. A minor landslide is also shown 500 m east of the main landslide area, which has displacement of 10 m in the central part. This result indicates that the PIV technique can precisely detect ground displacement or movement presented by aerial photographs. (For interpretation of the references to colour in this figure legend, the reader is referred to the web version of this article.)

above is related to how we decided the interrogation size during the process.

The second influence, appearance, is the most important of these three. The appearance of any image may be affected by many natural and artificial factors, such as the change of vegetation and artificial objects on the ground, the incident angle of the sun (or the time of taking photographs), the error from orthorectification and etc. Taking the results of Fig. 8A and B for example, they have different magnitude of displacement which seems to show a discrepancy. However, the discrepancy is due to the time when the photographs are being taken. Another important factor is that there are typhoons every year during summer time which have changed vegetations or even destroyed the morphology especially in mountain area in Taiwan. Therefore, if we want to obtain best results of the PIV analysis, selecting suitable images should be more carefully done. In this case, though typhoons have affected the Hongtsaiping area, most parts of the study area still remain their morphology. Therefore, typhoon events affected the PIV results slightly, because the magnitude of displacement of the Hongtsaiping landslide is much greater than the vegetation change due to typhoons.

Means of caculation	Results (pixels)
3-point Gauss Fit	44.7711
Least Squares Gauss Fit	45.0886
3-point Parabolic Fit	44.7778
Center-of-Mass Fit	42.4784
Whittacker Reconstruction	45.1436
Nonlinear Gaussian Peak Fit	45.0886

Fig. 11. The different results of six algorithms of peak detection provided from PIV. Various peak fit algorithms are available which recover the sub-pixel displacement of the value (peak) of cross-correlation. Least Square Gauss Fit is similar to the 3-point Gauss Fit but uses all eight points surrounding the maximum. Since Least Square Gauss Fit uses more data for the location of the peak, the noise in the result is generally less than with more simple fits. This peak fit method is suitable for most applications. The other algorithms are for wider correlation peaks or only need less data than Least Square Gauss Fit does, so we exploit Least Square Gauss Fit to approximate our results.

The RMS error of correlation algorithm depends on particle image displacement. Thus, if we want to get higher precision, the particle image displacement has to be very small. For our case of the Hongtsaiping landslide, the magnitude of displacement are 40–50 pixels (24–28 m), which have RMS error about 0.25–0.3 pixels (0.15–0.18 m). Comparing to the average magnitude of displacement 12 m, we have about 2% error in this case.

Although the PIV technique is not as precise as traditional geological fieldwork in small locations, it can provide wide-covered area analysis and unobvious trend of non-catastrophic landslides or creep in mountain area where researchers hardly arrive. Furthermore, PIV is also convenient and good at long term monitoring on non-catastrophic landslides or creep due to tectonically with periodically taking of images.

5. Conclusion

The horizontal magnitude of displacement in the Hongtsaiping landslide area is about 39.24–46.28 pixels (24–28 m), and the RMS error is about 0.3 pixels (0.18 m). The PIV analysis can precisely evaluate the behavior, including magnitude, direction

and area of non-catastrophic landslides or creep of rocks mass in small scale. With the data of monochromatic orthorectified aerial photographs which possess good appearance of ground objects, such as relatively hardly changeable objects of houses, towers and etc., PIV will show fine results. PIV also shows good results from creep or non-catastrophic landslides in towns or cities (Chan et al., 2004; Chen and Lee, 2005). Besides, the PIV analysis can only show horizontal changes, so we have to know the slope or dipping of the local beddings and to consider the efficiency of the topography in local study areas. On the other hand, the cross-correlation has evaluation deviation which is proportional to displacement, so the PIV analysis is not suitable for analysis of large displacement, but for small scale creep or non-catastrophic landslides. The PIV technique is a convenient tool to analyze wide-covered area and can be applied to long term monitoring of geological events.

Acknowledgements

We are grateful to two anonymous reviewers, Benoit Deffontaines and Shu-Kun Hsu for their constructive comments. The suggestions and discussions with Jacques Angelier and Jian-Cheng Lee are deeply appreciated. This research was supported by the National Science Council of Taiwan under grant No. NSC 94-2119-M-002-021 and the Central Geological Survey of the MOEA. This research was supported by the Taiwan Earthquake Research Center (TEC) funded through National Science Council (NSC). The TEC contribution number for this article is 00022.

References

Adrian, R.J., 1991. Particle imaging techniques for experimental fluid mechanics. Ann. Rev. Fluid Mech. 23, 261–304.

Angelier, J., Lee, J.-C., Chu, H.-T., Hu, J.-C., Lu, C.-Y., Chan, Y.-C., Lin, T.-J., Font, Y., Deffontaines, B., Tsai, Y.B., 2001. Le Séisme de Chichi (1999) et sa place dans l'orègene de Taiwan. C. R. Acad. Sci. Paris, Earth Planet. Sci. 333, 5–21.

Berthier, E., Vadon, H., Baratoux, D., Arnaud, Y., Vincent, C., Feigl, K.L., Rémy, F., Legrésy, B., 2005. Mountain glaciers surface motion derived from satellite optical imagery. Remote Sens. Environ. 95, 14–28. doi:10.1016/j.res.2004.11.005.

Casson, B., Delacourt, C., Allemand, P., 2005. Contribution of multi-temporal remote sensing images to characterize landslide slip surface — application to the La Clapière landslide (France). Nat. Hazards Earth Syst. Sci. 5, 425–437.

Chambon, G., Schmittbuhl, J., Corfdir, A., Vilotte, J.-P., Roux, S., 2003. Shear with comminution of a granular material: microscopic deformations outside the shear band. Phys. Rev., E 68, 011304.

Chan, Y.-C., Chou, S.-C., Lee, J.-C., 2004. Reconstruction of high-resolution horizontal displacement field using aerial photogrammetry and particle image velocimetry: an example from the Taiwan Chi-Chi Earthquake rupture area. AGU 2004 Fall Meeting.

Chen, R.-F., Lee, J.-C., 2005. Application of the particle image velocimetry (PIV) technique to obtain near-fault surface displacement field: a case study of the 2003, M_w=6.5, Chengkung earthquake in eastern Taiwan. Geodynamics and Environment in East Asia International Conference & 5th Taiwan–France Earth Science Symposium.

Chen, Y.-G., Chen, W.-S., Lee, J.-C., Lee, Y.-H., Lee, C.-T., Chang, H.-C., Lo, C.H., 2001a. Surface rupture of 1999 Chi-Chi Earthquake yields insights on active tectonics of central Taiwan. Bull. Seismol. Soc. Am. 91, 977–985.

Chen, W.-S., Huang, B.-S., Chen, Y.-G., Lee, Y.-H., Yang, C.-N., Lo, C.H., Chang, H.-C., Song, Q.-C., Huang, N.-W., Lin, C.-C., Sung, S.-H., Lee, K.-J., 2001b. 1999 Chi-Chi earthquake: a case study on the role of thrust-ramp structures for genera ting earthquake. Bull. Seismol. Soc. Am. 91, 986–994.

Chigira, M., Wang, W.N., Furuya, T., Kamai, T., 2003. Geological causes and geomorphological precursors of the Tsaoling landslide triggered by the 1999 Chi-Chi earthquake, Taiwan. Eng. Geol. 68, 259–273.

Delacourt, C., Allemand, P., Casson, B., Vadon, H., 2004. Velocity field of the "La Clapière'' landslide measured by the correlation of aerial and QuickBird satellite images. Geophys. Res. Lett. 31, L15619. doi:10.1029/2004GL020193.

Dominguez, S., Avouac, J.-P., Michel, R., 2003. Horizontal coseismic deformation of the 1999 Chi-Chi earthquake measured from SPOT satellite images: implications for the seismic cycle along the western foothills of central Taiwan. J. Geophys. Res. 108 (B2), 2083.

Fritz, H.M., 2002. Initial phase of landslide generated impulse waves. Dissertation of Swiss Federal Institute of Technology Zürich.

Hung, J.-J., 2000. Chi-Chi earthquake induced landslides in Taiwan. Earthq. Eng. Eng. Seismol. 2, 25–32.

Hung, J.-J., Lee, C.-T., Lin, M.-L., 2000. Tsao-Ling rockslides, Taiwan, catastrophic landslides: effects, occurrence, and mechanisms. Geol. Soc. Amer. Rev. Eng. Geol. 15, 91–115.

Kääb, A., 2002. Monitoring high-mountain terrain deformation from repeated air- and spaceborne optical data: examples using digital aerial imagery and ASTER data. ISPRS J. Photogramm. Remote Sens. 57, 39–52.

Kao, H., Chen, W.-P., 2000. The Chichi earthquake sequence: active out-of-sequence thrust faulting in Taiwan. Science 30, 2346–2349.

Landreth, C.C., Adrian, R.J., 1988. Electro-optical image shifting for particle image velocimetry. Appl. Opt. 27, 4216–4220.

Lecordier, B., Mouqallid, M., 1994. CCD recording method for cross-correlation PIV development in unstationary high speed flow. Exp. Fluids 17, 205.

Lee, J.-C., Chu, H.-T., Angelier, J., Chan, Y.-C., Hu, J.-C., Lu, C.-Y., Rau, R.-J., 2002. Geometry and structure of northern surface rupture of the 1999 M_w=7.6 Chi-Chi, Taiwan Earthquake: influence from inherited Fold Belt structures. J. Struct. Geol. 24, 173–192.

Lee, J.-F., Wei, C.-Y., Huang, C.-C., 2004. The Study of Hungtsaiping Landslide Using Digital Aerial Photogrametric Technique, pp. (5–1).

Liao, C.-W., Lee, C.-T., Liao, H.-W., 2002. Statistical Analysis of Factors Affecting Landslides Triggered by the 1999 Chi-Chi Earthquake, Taiwan, AGU 2002 fall Meeting Program, p. 258.

Lin, M.-L., Liao, H.-J., Ueng, Z.S., 2000. The geotechnical hazard caused by Chi-Chi earthquake. Proc. International Workshop on the September 21, 1999 Chi-Chi Earthquake, Taichung, Taiwan, pp. 113–123.

Meinhart, C.D., Wereley, S.T., Santiago, J.G., 1999. PIV measurements of a microchannel flow. Exp. Fluids. 414–419.

Rees, W.G., 2001. Physical Principles of Remote Sensing, 2nd ed. Cambridge University Press, Cambridge. (343).

Rhoály, J., Frigerio, F., Hart, D.P., 2002. Reverse hierarchical PIV processing. Meas. Sci. Technol. 13, 984–996.

Shou, K.-J., Wang, C.-F., 2003. Analysis of the Chiufengershan landslide triggered by the 1999 Chi-Chi earthquake in Taiwan. Eng. Geol. 68, 237–250.

Wei, J.-Y., Lee, J.-F., 2006. The application of digital aerial photography in the study of Hungtsaiping Landslide, Chungliao, Nantou County. Bull. Cent. Geol. Surv. 19, 39–59.

White, D.J., Take, W.A., Bolton, M.D., 2003. Soil deformation measurement using particle image velocimetry (PIV) and photogrammetry. Géotechnique 53 (7), 619–631.